

400 element ErAs:InGaAs/InGaAlAs superlattice power generator

Gehong Zeng, Je-Hyeong Bahk, John E. Bowers
Department of Electrical and Computer Engineering, University of California, Santa Barbara, CA 93106

Joshua M. O. Zide, Arthur C. Gossard
Materials Department, University of California, Santa Barbara, CA 93106

Yan Zhang, Rajeev Singh, Zhixi Bian and Ali Shakouri
Electrical Engineering Department, University of California, Santa Cruz, CA 95064

Woochul Kim, Suzanne Singer, Arun Majumdar
Department of Mechanical Engineering, University of California, Berkeley, CA 94720

ABSTRACT

We report the fabrication and characterization of thin film power generators composed 400 p- and n-type ErAs:InGaAs/InGaAlAs superlattice thermoelectric elements. The thermoelectric elements incorporate erbium arsenide metallic nanoparticles into the semiconductor superlattice structure to provide charge carriers and create scattering centers for phonons. 10 μm p- and n-type InGaAs/InGaAlAs superlattices with embedded ErAs nano-particles were grown on InP substrates using molecular beam epitaxy. Thermal conductivity values were measured using the 3ω method and cross-plane Seebeck coefficients were determined using Seebeck device test patterns. 400 element ErAs:InGaAs/InGaAlAs thin film power generators were fabricated from superlattice elements 10 μm thick and 200 $\mu\text{m} \times 200 \mu\text{m}$ in area. The output power was 4.7 milliwatts for an external electrical load resistor of 150 Ω at about 80 K temperature difference drop across the generator. We discuss the limitations to the generator's performance and provide suggestions for further improvement.

INTRODUCTION

The performance of thermoelectric generators is largely dependent on the material figure-of-merit $Z = \alpha^2 \sigma / \kappa$, where α is the material Seebeck coefficient, σ is the electrical conductivity and κ is the thermal conductivity. A large figure-of-merit ZT is necessary for high power densities and high efficiency. A number of approaches have been pursuing to improve the performance of solid state power generators[1-5]. A lot of research has been done to improve various material thermoelectric properties beyond bulk materials or alloys using superlattice structures[6-12]. Heterostructures can enhance the thermoelectric device performance by the selective emission of hot carriers above the potential barrier through thermionic emission[13]. Low dimensional structures could overcome the efficiency barriers imposed by the physical limit of conventional bulk materials[14-17]. Superlattice interfaces provide phonon scattering centers to reduce the cross-plane thermal conductivity[18]. To achieve high thermoelectric conversion efficiency[19] we suggested using non-planar barriers and embedded quantum dot structures. The incorporation of erbium arsenide metallic nanoparticles into the

InGaAs/InGaAlAs superlattice can provide both charge carriers and create scattering centers for phonons. In this paper, we report on the fabrication and characterization of 400 element thin film array power generators using these ErAs:InGaAs/InGaAlAs superlattices.

MATERIAL GROWTH AND CHARACTERIZATION

ErAs:InGaAs/InGaAlAs superlattice samples were grown on (100) InP substrates using a Varian Gen II molecular beam epitaxy (MBE) system[20]. Erbium particles are randomly distributed through the InGaAs layers, which provide $2 \times 10^{18} \text{ cm}^{-3}$ doping. Silicon co-doping was used for the n-ErAs:InGaAs/InGaAlAs sample; the p-ErAs:InGaAs/InGaAlAs sample was co-doped with Be.

The in-plane Seebeck coefficient was measured for both n-ErAs:InGaAs/InGaAlAs and p-ErAs:InGaAs/InGaAlAs using samples grown on a semi-insulating InP substrate. The measurements were done by using two thermoelectric coolers to build up a temperature difference across the test sample plates about $5 \text{ mm} \times 15 \text{ mm}$. By measuring the output voltage at different temperature differences across the sample, the in-plane Seebeck coefficients were obtained by a linear curve fitting of the voltage versus temperature difference data. The in-plane Seebeck coefficients of both n and p ErAs:InGaAs/InGaAlAs superlattices are shown in figure 1.

The cross-plane and in-plane Seebeck coefficients of a superlattice are usually different due to the electron filtering effects of superlattice structure. To determine the cross plane Seebeck coefficient, four n-ErAs:InGaAs/InGaAlAs superlattice samples with the same structures but different dopings were grown on conductive InP substrates using MBE. The effective doping for the four samples is 2×10^{18} , 4×10^{18} , 6×10^{18} and

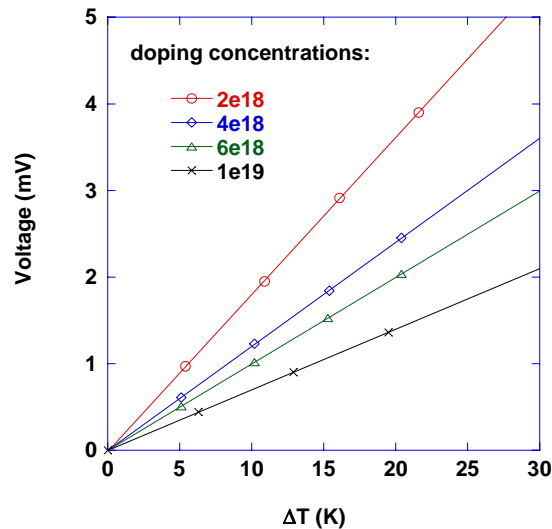


Figure 1. The in-plane Seebeck coefficients were measured 181, 120, 100 and $70 \mu\text{V/K}$ for n-ErAs:InGaAs/InGaAlAs samples grown on insulating InP with the doping concentration of 2×10^{18} , 4×10^{18} , 6×10^{18} and $1 \times 10^{19} \text{ cm}^{-3}$ respectively.

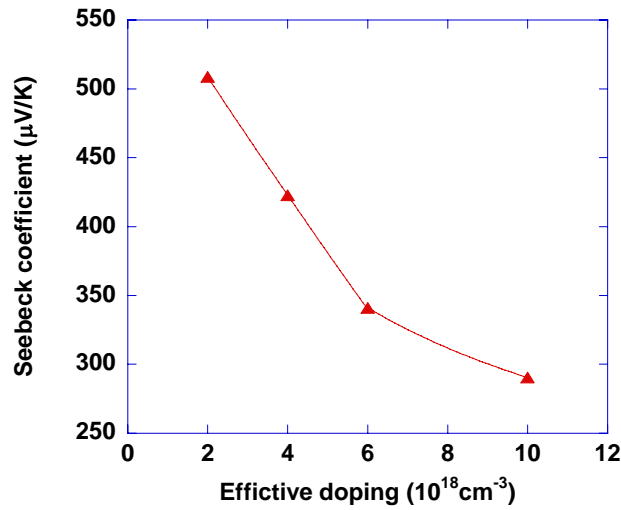


Figure 2. Measurement results of cross-plane Seebeck coefficients of n-ErAs:InGaAs/InGaAsAs superlattice samples with different doping concentrations.

$1 \times 10^{19} \text{ cm}^{-3}$ respectively. The cross-plane Seebeck coefficients for the four samples were measured for 509, 422, 341 and 290 $\mu\text{V/K}$ respectively at room temperature using device test patterns[21]. Figure 2 shows the cross-plane Seebeck coefficients for an n-ErAs:InGaAs/InGaAlAs superlattice versus doping concentration. The thermal conductivity is a key factor for achieving a high generator performance. Reducing the thermal conductivity results in a greater temperature difference across the thermoelectric elements and provides more output power with higher efficiency. The cross-plane

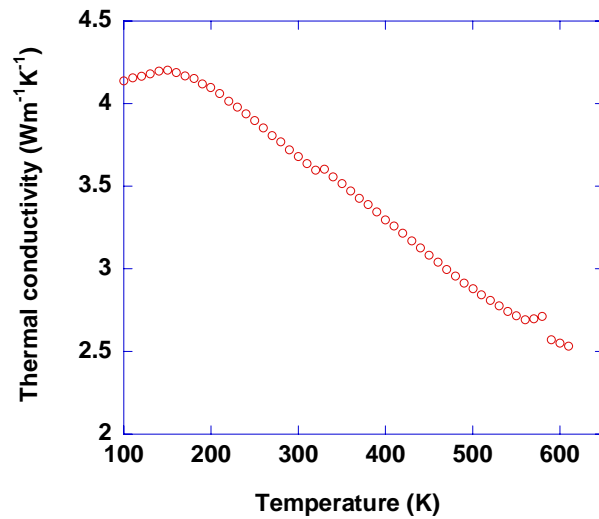


Figure 3. The thermal conductivity measurement results for ErAs:InGaAs/InGaAlAs superlattice using 3w method.

thermal conductivity of ErAs:InGaAs/InGaAlAs superlattices were measured using the 3ω method[22], and the results are shown in figure 3. The thermal conductivity values are less than $3.68 \text{ Wm}^{-1}\text{K}^{-1}$ when working temperatures are 300 K and above. Decreasing thermal conductivity with increasing temperature indicates Umklapp scattering is dominant in the measurement temperature range. The interface phonon scattering produced by the superlattice heterostructure interface and ErAs nanoparticles played an important role in the thermal conductivity reduction from the value $\sim 5.5 \text{ Wm}^{-1}\text{K}^{-1}$ of InGaAs alloy.

DEVICE FABRICATION AND MEASUREMENTS

The processing of ErAs:InGaAs/InGaAlAs superlattice element array is compatible with integrated circuit fabrication process. Mesas $13 \mu\text{m}$ high and $200 \mu\text{m} \times 200 \mu\text{m}$ in area were formed by dry etching the InP substrate, and contact and bonding metal layers were deposited on top of these elements using electron beam evaporation. Low contact resistance at the metal/semiconductor interface is a key factor to the thin film generator performance. Ni/Ge metallization was used to make ohmic contact to the superlattice elements. Specific contact resistivity on the order of $10^{-7} \Omega\cdot\text{cm}^2$ was measured from room temperature up to $250 \text{ }^\circ\text{C}$ using transfer length method (TLM). The processed element arrays are shown in figure 4.

The array generator was formed via flip-chip bonding: A 200 element n-ErAs:InGaAs/InGaAlAs element array and a 200 element p-ErAs:InGaAs/InGaAlAs are bonded to $650 \mu\text{m}$ thick upper and lower AlN plates respectively. The InP substrates were removed by wet etching to form n or p thin film element arrays as shown in figure 5.

These 200 element n or p arrays on the AlN plates were all superlattice mesas $10 \mu\text{m}$ high. Contact metals of Ni/Ge were deposited on top of the array elements, and then a p-type array on upper AlN plate and an n-type array on lower AlN plate were bonded together to form the 400 element array generator as shown in figure 6.

Output power on the temperature difference across the sample was measured with electrical loads from 1Ω to 2000Ω , and figure 7 shows the measurement results. The maximal output power measured was about 5 mW on an external resistant R_L of 150Ω . The results of output power varying with different external resistant loads R_L are shown in figure 8.

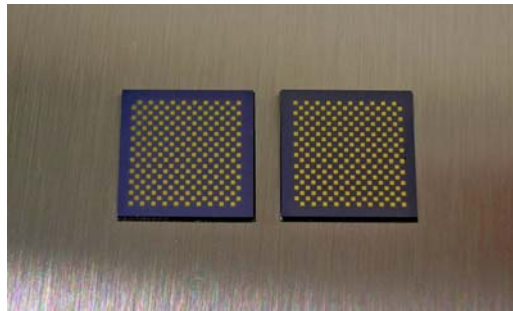


Figure 4. Processed n and p ErAs:InGaAs/InGaAlAs chips, each containing 200 elements

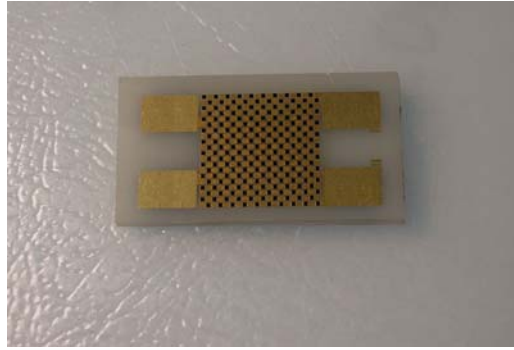


Figure 5. 200 n-ErAs:InGaAs/InGaAlAs elements were bonded on an AlN plate after the InP substrate was removed.

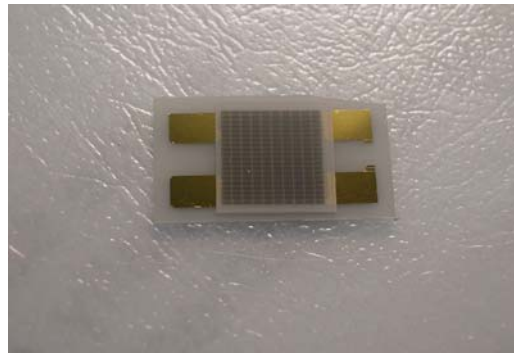


Figure 6. A photo of 400 superlattice element array power generator, bonded together with a 200 n-ErAs superlattice elements on lower AlN plate and 200 p-ErAs superlattice elements on upper AlN using filp-chip bonding method.

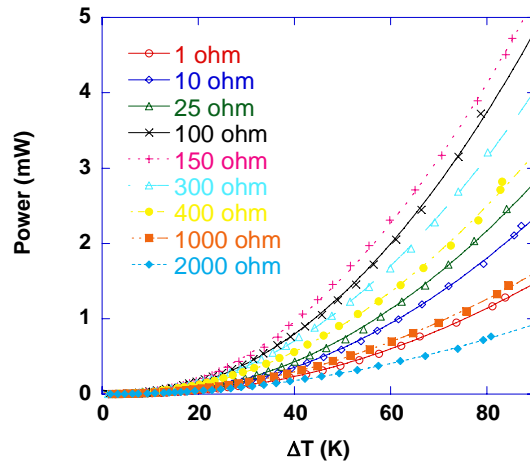


Figure 7. Measurement results for a 400 element superlattice array generator with the temperature difference ΔT across the whole package up to 80K and external load resistance ranging from 1Ω to 2000Ω .

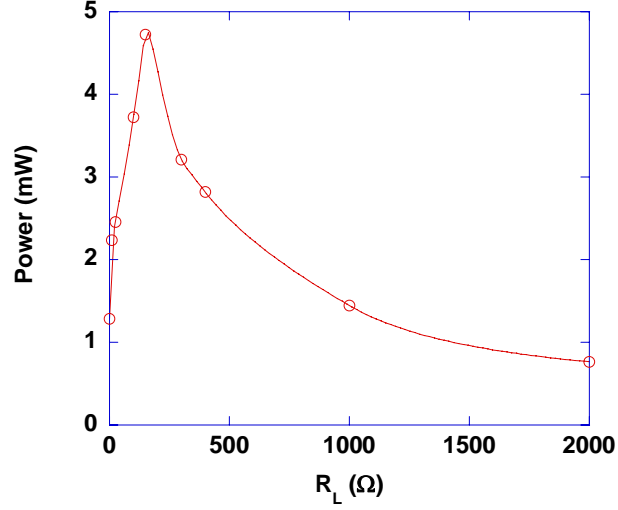


Figure 8. The output power was measured with different external resistant loads R_L when the temperature different dropping across the whole package is at 80K.

DISCUSSIONS

The output power can be expressed as $P = R_L \left(\frac{\alpha \cdot \Delta T_e}{R_L + r} \right)^2$, where ΔT_e is the temperature drop across the superlattice thin film elements, α is the Seebeck coefficient, R_L is the external electrical load resistance, and r is the internal resistance of the module. Thermal simulations show that almost half of the temperature drop was across the two AlN plates each 140 μm thick, which presents a limitation to the generator's performance. To some extent this can be solved either by using thinner AlN plates or by using a higher thermal conductivity material, such as diamond, for the package plates while and increasing the superlattice thickness. The internal parasitic resistance loss, which includes resistance of internal metal connections and the contact resistance, is also a limitation. Because the thin film superlattice elements are only a few microns thick, the contact resistance and/or internal connection metal layers may become a dominant factor. Keeping the contact resistance low and further reducing the resistance of the internal connections are necessary. Fundamentally, the generator performance is determined by the thermoelectric ZT of the element material. A superlattice structure provides more opportunities to engineer electrical and thermal properties. Our measurements on the thermal conductivity, and cross-plane Seebeck coefficient of ErAs:InGaAs/InGaAlAs superlattice samples show that the incorporation of erbium arsenide metallic nanoparticles into the semiconductor superlattice structure provides an attractive way for the enhancement of the material thermoelectric properties. With the improvement of material properties, and the optimization of the generator structure and packaging design, a superlattice thin film generator with an output power density of over 1 W/cm^2 should be possible when working with heat sources of about 700K.

CONCLUSIONS

In summary, 400 element ErAs:InGaAs/InGaAlAs superlattice thin film array generators were fabricated. An output power of over 4.7 mW was measured on an external load resistor of 150 Ω when the temperature drop across the whole device package was 80K. Each superlattice element is 10 μm thick and 200 $\mu\text{m} \times 200 \mu\text{m}$ in area size. The superlattices were grown using molecular beam epitaxy, and characterized by measuring the cross plane thermal conductivity and Seebeck coefficients. With the optimization of superlattice property, generator and packaging design, an output power over 1 W/cm^2 should be achievable.

ACKNOWLEDGEMENTS

This work is supported by the Office of Naval Research Thermionic Energy Conversion Center MURI managed by Dr. Mihal E. Gross.

REFERENCES

1. G. J. Snyder, J. R. Lim, C. K. Huang, and J. P. Fleurial, "Thermoelectric microdevice fabricated by a MEMS-like electrochemical process," *Nature Materials*, vol. 2, pp. 528-531, 2003.
2. Z. H. Dughaish, "Lead telluride as a thermoelectric material for thermoelectric power generation," *Physica B-Condensed Matter*, vol. 322, pp. 205-223, 2002.
3. I. H. Kim, "(Bi,Sb)(2)(Te,Se)(3)-based thin film thermoelectric generators," *Materials Letters*, vol. 43, pp. 221-224, 2000.
4. D. M. Rowe, *CRC handbook of thermoelectronics*. New York: CRC Press, 1995.
5. G. Zeng, J. E. Bowers, Y. Zhang, and A. Shakouri, "SiGe/Si superlattice power generators," *24th International Conference on Thermoelectrics*, 2005.
6. R. Venkatasubramanian, E. Siivola, T. Colpitts, and B. O'Quinn, "Thin-film thermoelectric devices with high room-temperature figures of merit," *Nature*, vol. 413, pp. 597-602, 2001.
7. T. E. Humphrey and H. Linke, "Reversible thermoelectric nanomaterials," *Physical Review Letters*, vol. 94, pp. 096601-4, 2005.
8. L. D. Hicks and M. S. Dresselhaus, "Effect of Quantum-Well Structures on the Thermoelectric Figure of Merit," *Physical Review B*, vol. 47, pp. 12727-12731, 1993.
9. T. C. Harman, P. J. Taylor, M. P. Walsh, and B. E. LaForge, "Quantum dot superlattice thermoelectric materials and devices," *Science*, vol. 297, pp. 2229-2232, 2002.
10. D. G. Cahill, W. K. Ford, K. E. Goodson, G. D. Mahan, A. Majumdar, H. J. Maris, R. Merlin, and S. R. Phillpot, "Nanoscale thermal transport," *Journal of Applied Physics*, vol. 93, pp. 793-818, 2003.
11. T. Koga, X. Sun, S. B. Cronin, and M. S. Dresselhaus, "Carrier pocket engineering to design superior thermoelectric materials using GaAs/AlAs superlattices," *Applied Physics Letters*, vol. 73, pp. 2950-2952, 1998.

12. T. Koga, X. Sun, S. B. Cronin, and M. S. Dresselhaus, "Carrier pocket engineering applied to "strained" Si/Ge superlattices to design useful thermoelectric materials," *Applied Physics Letters*, vol. 75, pp. 2438-2440, 1999.
13. A. Shakouri and J. E. Bowers, "Heterostructure integrated thermionic coolers," *Applied Physics Letters*, vol. 71, pp. 1234-1236, 1997.
14. M. J. Kelly, *Low-dimensional semiconductors : materials, physics, technology, devices*. New York: Oxford University Press, 1995.
15. V. A. Markel and T. F. George, *Optics of Nanostructured Materials (Wiley Series in Lasers and Applications)*: Wiley-Interscience, 2000.
16. T. M. Tritt, "Recent trends in thermoelectric materials research III - Semiconductors and semimetals - Preface," *Recent Trends in Thermoelectric Materials Research Iii*, vol. 71, pp. ix-xiv, 2001.
17. L. D. Hicks and M. S. Dresselhaus, "Thermoelectric Figure of Merit of a One-Dimensional Conductor," *Physical Review B*, vol. 47, pp. 16631-16634, 1993.
18. S. T. Huxtable, A. R. Abramson, C. L. Tien, A. Majumdar, C. LaBounty, X. Fan, G. H. Zeng, J. E. Bowers, A. Shakouri, and E. T. Croke, "Thermal conductivity of Si/SiGe and SiGe/SiGe superlattices," *Applied Physics Letters*, vol. 80, pp. 1737-1739, 2002.
19. D. Vashaee and A. Shakouri, "Improved thermoelectric power factor in metal-based superlattices," *Physical Review Letters*, vol. 92, pp. 106103/1, 2004.
20. J. M. Zide, D. O. Klenov, S. Stemmer, A. C. Gossard, G. Zeng, J. E. Bowers, D. Vashaee, and A. Shakouri, "Thermoelectric power factor in semiconductors with buried epitaxial semimetallic nanoparticles," *Applied Physics Letters*, vol. 87, pp. 112102, 2005.
21. G. Zeng, J. E. Bowers, Y. Zhang, A. Shakouri, J. M. Zide, A. C. Gossard, W. Kim, and A. Majumdar, "ErAs/InGaAs superlattice Seebeck coefficient," *24th International Conference on Thermoelectrics*, 2005.
22. D. G. Cahill, "Thermal-Conductivity Measurement from 30-K to 750-K - the 3-Omega Method," *Review of Scientific Instruments*, vol. 61, pp. 802-808, 1990.